Simulations on the Nonlinear Mode Coupling in Multiple-scale Drift-type Turbulence with Coherent Flow Structures

Jiquan Li 1,2), K. Uzawa 2), Z. Lin 3), Y. Kishimoto 2), N. Miyato 4), T. Matsumoto 4), J.Q. Dong 1)

1) Southwestern Institute of Physics, P.O. Box 432, Chengdu, Sichuan 610041, China
2) Graduate School of Energy Science, Kyoto University, 611-0011 Gokasho, Uji, Japan
3) Department of Physics and Astronomy, University of California, Irvine, California 92697
4) Fusion Research and Development Directorate, JAEA, Naka, Ibaraki 311-0193, Japan

e-mail contact of main author: lijq@energy.kyoto-u.ac.jp

Abstract: The dynamics of secondary, anisotropic coherent structures behaving as a stationary wave, including zonal/mean flows, streamers and low-frequency long wavelength fluctuations, in multiple-scale turbulence in tokamak plasmas is investigated by performing 3D simulations as well as 2D modeling analyses. The role of nonlinear mode coupling is specifically discussed as a ubiquitous principal interaction mechanism in the dual processes of the generation and back-action of secondary structures on ITG and ETG turbulence. Here two new results are evidently presented on the importance of the mode coupling interaction: (1) While secondary zonal flows and long wavelength modes are generated through nonlinear mode coupling, the same back-action process can deform the spectral distribution in inertia range from the power-law scaling into an exponential-law dependence. The turbulence may be reduced due to the local and/or nonlocal free energy transfer to stable region. (2) Streamer-like long wavelength fluctuations driven by the most unstable ETG modes, can saturate slab ETG turbulence through producing a k_y -mode coupling that corresponds to the toroidal mode coupling in tokamak plasma, suggesting a low ETG fluctuation level and electron transport. Furthermore, the effect of ITG generated zonal flows regarded as a wave-type mean flow on the generation of zonal flows in ETG turbulence is also discussed with an emphasis on the role of nonlinear mode coupling.

1. Introduction

Plasma fluctuations in magnetically confined devices, such as the magnetohydrodynamic (MHD) and drift-type turbulence in tokamaks, possess multiple spatio-temporal scales and spectral anisotropy due to the richness of linear and/or nonlinear instabilities. Multi-scale fluctuations may coexist and interplay each other in a highly turbulent environment so that the characteristics of individual turbulence may be affected, even changed. This important issue has attracted intensive attention recently[1-5]. Typically, ion scale fluctuations such as ion temperature gradient(ITG) modes may coexist with the electron scale counterpart ETG turbulence and also larger scale MHD mode, the complex nonlinear interaction could make the electron and ion transport coupled closely. On the other hand, coherent anisotropic flow structures, such as poloidally elongated zonal flows and radially extended streamers as well as low frequency long wavelength generalized Kelvin-Helmholtz (GKH) fluctuations[6-12], are generated nonlinearly as a secondary component. These large-scale structures are generally characterized by approximately periodic spatial variation. It has been noticed that such *wave-type flow structures* can not only provide a local shearing decorrelation effect on the ambient or adjacent turbulence[13], but also behave as a stationary wave in a turbulence bath. The former dynamics is similar to smooth mean sheared flows. The latter characteristics should be understood through the nonlinear mode coupling[3,4,14-17].

Here our focus is on *the dynamics of coherent flow structures as a stationary wave interplaying with turbulent fluctuations* in ITG or ETG turbulence. Through the ubiquitous nonlinear mode coupling,

these coherent structures are generated as a beat wave or a modulational instability. Meanwhile, they act back on the turbulence and transfer locally or nonlocally the free energy to the short wavelength, highly dissipated region so that the fluctuations may be stabilized, even saturated. Three aspects related to such dual processes will be addressed based on 3D simulations and 2D modeling analysis: (1) Spectral characteristics on the nonlinear mode coupling due to the dynamics of secondary flow structures. (2) Role of streamer-like long wavelength fluctuations in ETG saturation; (3) Effects of wave-type mean flow on the zonal flow generation in microturbulence.

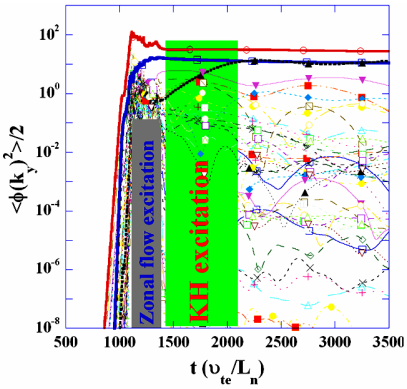

Fig.1 Time evolution of ETG turbulence in 2D modeling simulation with weak magnetic shear. The red, blue and blank solid curves indicates of the energy of total, zonal flow and KH modes, respectively. $\hat{s}=0.1$, $\eta_e=5.5$, $\mu_\perp=1.5$, $L_x=400\rho_e$, $L_y=160\pi\rho_e$.

2. Spectral Characteristics in the System of Turbulence and Flow Structures

To elucidate the principal interaction mechanism on the generation of secondary structures and the back-action on turbulence, an extended, forced Hasegawa-Mima(FHM) turbulence model is first developed to analyze the nonlinear mode coupling with high-resolution simulation. Different from conventional HM turbulence with a constraint of energy conservation, this free energy system, which includes linear ETG driving force and damping sink, ensures the sufficient spectral modulation of turbulence due to the back-action of secondary structures through mode coupling. Afterwards, 3D ETG and ITG simulations are performed to analyze the spectral characteristics of turbulence due to the dynamics of secondary flow structures.

2.1. Forced HM Turbulence and Modeling Simulation.

Note that HM turbulence has been extensively applied to analyze the generation of the zonal flows and streamers based on a modulation instability of four-wave interaction in ITG or ETG turbulence. ETG turbulence is a typical HM-type fluctuation[18], in which the modeling equation is the lowest order version of fluid ETG turbulence. i.e.,

$$(1-\nabla_\perp^2)\partial_t\phi=\partial_y\phi+[\phi,\nabla_\perp^2\phi] \quad , \tag{1}$$

where the Poisson blanket expresses the $\vec{E}\times\vec{B}$ nonlinearity. Due to the back-action of zonal flows, turbulent ETG spectra are determined by the balance among the linear driving and nonlinear damping as well as the impact of the secondary structures. Hence, an extended HM turbulence model is advanced to include the linear ETG driving and sink terms, i.e.,

$$(1-\nabla_\perp^2)\partial_t\phi=\partial_y\phi+[\phi,\nabla_\perp^2\phi]+K\nabla_\perp^2\partial_y\phi+\nabla_{//}\upsilon_{//}-\mu_\perp\nabla_\perp^4\phi \quad , \tag{2}$$

$$\partial_t\upsilon_{//}=\nabla_{//}(\phi-p_e)+\mu_\perp\nabla_\perp^2\upsilon_{//} \quad , \tag{3}$$

$$\partial_t p_e=-K\partial_y\phi-\Gamma\nabla_{//}\upsilon_{//}-(\Gamma-1)\sqrt{8/\pi}\,|k_{//}|(p_e+\phi)+\mu_\perp\nabla_\perp^2 p_e \quad , \tag{4}$$

with $K=1+\eta_e$. The notation and normalization are conventional as in [19,20]. This model excludes the nonlinearity from fluctuating parallel velocity and pressure so that it is only used to study the turbulence structure and flow dynamics as HM turbulence does.

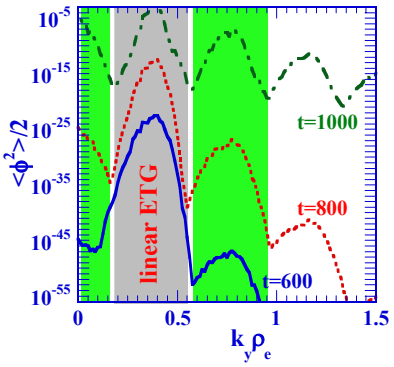

Fig.2 k_y spectral evolution before ETG saturation in 2D gyrofluid ETG modeling simulation. $\hat{s}=0.1$, $\eta_e=5.5$, $\mu_\perp=1.5$, $L_x=200\rho_e$, $L_y=160\pi\rho_e$. Green-marked shows GKH excitation and high k_y components due to nonlinear mode coupling.

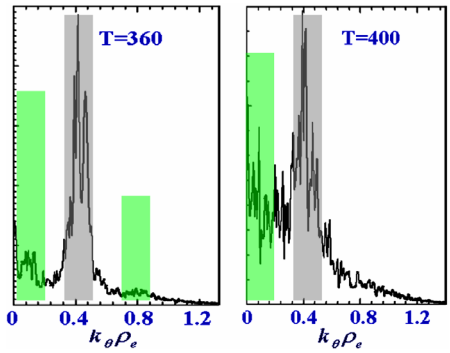

Fig.3 k_θ spectral evolution before ETG saturation in 3D gyrokinetic particle simulation using GTC code. $\hat{s}\approx 0.1$, $L_T=2.2$, $L_n=6.9$, $a/R=0.345$, $a/\rho_e=240$. Grey-marked indicates the spectral distribution of linear ETG modes.

Now 2D high-resolution simulations are performed for different magnetic shears. Fig.1 plots the time evolution of potential energy of k_y components in the simulation with $\hat{s}=0.1$. It shows that the zonal flow generation is enhanced after ETG saturation and limited finally by long wavelength KH excitation. The quasi-steady state is sustained by the coupling of ETG fluctuations, zonal flows and KH modes. The time evolution of complex interaction can be roughly divided into four phases: linear ETG growth with spectral peak $k_y\approx 0.4$ and GKH generation (I. t<1000); ETG saturation and zonal flow enhancement (II. 1000< t <14000); zonal flow saturation and linear excitation of KH mode with $k_y\approx 0.1$ (III. 1300<t <2000) and the quasi-steady state (IV. t >2000). In Phase I, the zonal flows accompanying with low k_y GKH modes are excited due to a three-wave interaction ($k_{y1}-k_{y2}=k_{yq}$, where subscript q denotes the secondary component and 1 and 2 are the most unstable ETG modes) or a weak modulation instability as shown in Fig.2. Meanwhile, the upper counterpart is also generated under the resonance condition $k_{y1}+k_{y2}=k_{yq}$. These secondary structures are commonly observed in our 2D and 3D gyrofluid ETG simulations. They also appear in globe gyrokinetic particle simulation of ETG turbulence using the GTC code as shown in Fig.3. By performing spectral analysis of k_x in 2D gyrofluid simulation, Figs. 4(a) and 4(b) display clearly 4-wave modulation interaction ($k_{x1}\pm k_{xq}=k_{x2}$) in phase II and 3-wave mode coupling ($k_{x1}+k_{xq}=k_{x2}$) in phase III between zonal flows and ETG fluctuations, respectively. The former reflects the well-known mechanism of zonal flow generation. The latter may uncover the primary mechanism of the back-action of zonal flows on the ambient turbulence through nonlinear mode coupling. This spectral relation is also observed in the simulation with higher shear, as shown in Fig.5. It is found that the spectral peak and width of the zonal flows increase with stronger magnetic shear. This tendency is projected to the location and width of spectral hump under the condition $k_{x1}+k_{xq}=k_{x2}$. For the evolution of k_y spectra from phase II to IV, it shows an explicit transition from a power-law dependence into an exponential-law scaling due to the excitation of KH mode, as shown in Fig. 6. It is speculated that the back-action of KH mode on the ETG turbulence through mode coupling may provide a driving force in the inertial range to modify the usual Kolmogorov-type spectrum. A similar exponential-law k_θ spectrum is also measured just after ETG saturation in gyrokinetic particle simulation using GTC code, in which pronounced secondary structures are generated, similar to that in Fig.3.

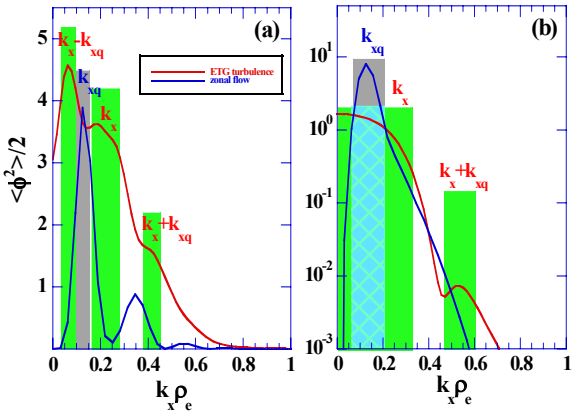

Fig.4 Radial spectra of ETG and zonal flows at t=1200 (a) and t=1500 (b) in Fig.1.

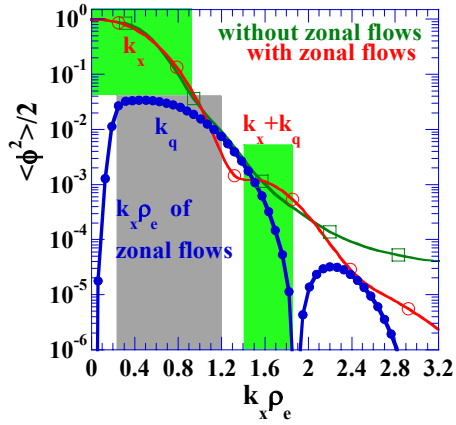

Fig.5 Radial spectra of ETG and zonal flows in similar simulation with shear $\hat{s}=0.8$. The green curve for the case without zonal flows is plotted for comparison.

2.2. Spectral Characteristics in 3D ETG and ITG Simulations

Motivated by the observations in 2D modeling simulations, 3D gyrofluid ETG and ITG simulations have been performed with and without zonal flow excitation for comparison to further investigate the spectral deformation due to the back-action of zonal flows through nonlinear mode coupling[12,20]. Note that the zonal flow intensity is distinctly different in ITG and ETG turbulence due to the different response to zonal flows by the adiabatic component, 3-field gyrofluid models of electrostatic slab ETG and ITG turbulence with corresponding electron or ion scale normalization are applied. Weak magnetic shear and steep temperature gradient are chosen in ETG simulation as in the 2D case to enhance the zonal flow generation. Fig.7 plots the k_x spectra of ETG turbulence in the quasi-steady state for two cases with and without zonal flow excitation, displaying different spectral dependence. A power-law spectral relation $\phi^2(k_x) \propto k_x^{-\alpha}$ is measured with $\alpha \approx 6.31$ in the simulation without zonal flows. The index is approximately the same as the analytical result $\alpha \approx 6.29$ based on a shell model of HM turbulence[21]. Such spectral distribution principally results from the enstrophy forward cascade and energy inverse cascade of the turbulence. However, an approximate exponential-law scaling $\phi^2(k_x) \propto e^{-\sigma k_x}$ with $\sigma \approx 3.5$ is measured in the simulation with enhanced zonal flows, as indicated by the inset in Fig.7. It is observed that the decay rate of k_x spectrum decreases in the interval $1 \le k_x\rho_e \le 2$. This is because the wavenumber of self-generated zonal flows is slightly smaller than or comparable to the ETG mode so that the notable modification of k_x spectrum may occur in this range.

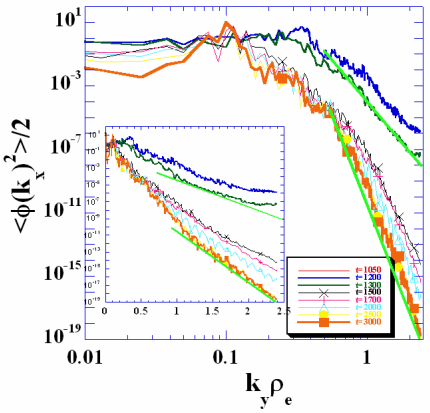

Fig.6 Time evolution of k_y spectra in Fig.1. Inset is the same plot with linear-scale x-axis. Straight lines are only for the reference of some scaling. It exhibits a transition of spectral scaling due to KH mode dynamics.

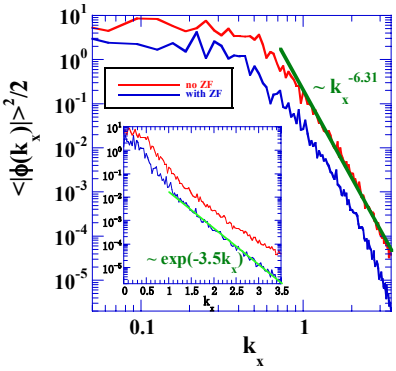

Fig.7 Radial spectra in 3D slab ETG simulations with and without zonal flows. Inset is the same plot with linear-scale x-axis. $\eta_e = 6$, $\hat{s} = 0.1$, $\mu_\perp = 0.5$.

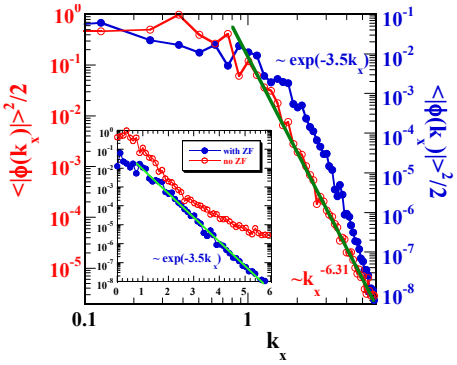

Fig.8 Radial spectra in 3D slab ITG simulations similar to Fig.7. Inset is the same plot with linear-scale x-axis. $\eta_i = 2.5$, $\hat{s} = 0.2$, $\mu_\perp = 0.1$.

In 3D ITG simulations, similar spectral characteristics are observed in the corresponding cases. However, the transition of spectral dependence of k_x becomes much explicit from the power-law $\phi^2(k_x) \propto k_x^{-6.3}$ to the exponential-law $\phi^2(k_x) \propto e^{-3.0k_x}$ scaling due to relatively robust zonal flow dynamics. The difference of spectral decay rate due to the back-action of zonal flows is compared in Fig.8. *It clearly shows that the nonlinear mode coupling between zonal flows and unstable ITG modes provides a driving force to deform the spectral scaling.* Such mechanism involving the nonlinear mode coupling should be different from the usual flow shearing decorrelation which may locally widen the radial spectral distribution. This feature is specifically identified in the interaction between ITG turbulence and ETG generated zonal flows, in which the ETG zonal flows possess a larger k_x than ITG turbulence so that pronounced spectral humps with $\Delta k_x \approx 2.0$ appear in high k_x region due to the nonlocal mode coupling[3,4].

3. Role of streamers and secondary long wavelength fluctuation in ETG saturation

Although several ETG turbulence simulations observed streamers, which are expected to cause high electron transport based on mixing-length argument, different electron transport levels are measured in these simulations [11,12,16,22,23]. These results motivate us to understand the overall role of the streamers and the possible effects of the secondary long wavelength modes in ETG saturation. To focus on the basic mechanism of the interaction, 3D electrostatic slab gyrofluid ETG simulation with periodic boundary conditions is performed to analyze the spectral evolution. Fig.9 plots the evolution of turbulent potential energy for each k_y. In the early linear phase, the component with $k_y = 0.1$, which is the beat wave of the most unstable modes ($k_y = 0.5 \sim 0.6$), grows quickly. As the amplitudes of the most unstable modes and the large-scale beat wave increase exponentially, other components drastically increase faster than an exponential growth in time. This process seems to signify that the nonlinear mode coupling between the beat wave $k_y = 0.1$ and the most unstable modes may provide an additional driving force for other components. Afterwards, the ETG fluctuation is saturated at a lower level. A modulational instability analysis with two pump waves based on HM turbulence model has been done for the generation of long wavelength beat wave $k_y = 0.1$ in Fig.9. A weak instability can occur near $k_x \approx 0.3$ and $k_x \approx 0.8$. To inspect the possible role of this secondary structure in ETG saturation, a streamer-like structure $\phi_s = \phi_{s0}(t)\cos(k_s y)$ with $k_s << 1$ as a limit case ignoring k_x dependence is sampled for simplicity to analyze the mode coupling between secondary structure and ETG modes. When the streamer-like structure is imposed in a linear slab ETG environment, it can

produce a k_y-mode coupling as follows

$$\partial_t(1-\nabla_\perp^2)\phi^{k_y} = (1+K\nabla_\perp^2)\partial_y\phi^{k_y} + \nabla_{//}\upsilon_{//}^{k_y} - ik_s\phi_s\partial_x\nabla_\perp^2(\phi^{k_y+k_s} - \phi^{k_y-k_s})/2 - \mu_\perp\nabla_\perp^4\phi^{k_y} \quad , \tag{5}$$

$$\partial_t\upsilon_{//}^{k_y} = \nabla_{//}(\phi^{k_y} - p_e^{k_y}) + ik_s\phi_s\partial_x(\upsilon_{//}^{k_y+k_s} - \upsilon_{//}^{k_y-k_s})/2 + \mu_\perp\nabla_\perp^2\upsilon_{//}^{k_y} \quad , \tag{6}$$

$$\partial_t p_e^{k_y} = -K\partial_y\phi^{k_y} - \Gamma\nabla_{//}\upsilon_{//}^{k_y} + \sqrt{32/9\pi}\,|k_{//}|(p_e^{k_y} + \phi^{k_y}) + ik_s\phi_s\partial_x(p_e^{k_y+k_s} - p_e^{k_y-k_s})/2 + \mu_\perp\nabla_\perp^2 p_e^{k_y} \, . \tag{7}$$

This set of coupled equations describes how the long wavelength structure such as the streamer-like mode interacts with ETG modes. It is expected that this mode coupling may become stronger for a realistic long wavelength structure with radial dependence. Note that the k_y-mode coupling in a slab corresponds to the toroidal mode coupling in a tokamak plasma[16,17]. Hence, it is deduced that the long wavelength structure can couple the most unstable modes with the damped modes so that the ETG fluctuation is stabilized. This analytical result is confirmed numerically by imposing a streamer-like structure with finite constant amplitude in a pure linear 2D slab ETG environment. It is observed that all k_y components have a same growth rate due to the k_y-mode coupling, which is smaller than that of the most unstable mode in the case of $\phi_s = 0$.

To investigate the role of this long wavelength mode in ETG saturation, a time-depended streamer-like structure with twice growth rate of the most unstable components is imposed in linear ETG fluctuations. This might be similar to the evolution of the beat wave $k_y = 0.1$ in Fig.9. Calculations show that the ETG fluctuations can be saturated at a similar fluctuation level in Fig.9 only through the dynamics of streamer-like structure, as shown in Fig.10. All k_y components besides the most unstable ones dramatically increase before the ETG saturation. The saturation amplitude decreases with stronger streamer intensity or/and small real frequency. The comparison of Fig.10 and Fig.9 shows that the saturation processes and levels of ETG modes are almost the same, suggesting that the secondary long wavelength structures can saturate ETG turbulence through a nonlinear mode coupling. The spectral evolution in the simulation of Fig.9 visibly displays the generation of secondary long wavelength mode and its coupling with ETG modes, finally, the spectral connection and mixture with primary ETG modes, as shown in Fig.11. This result indicates that *although the streamer-like structures are expected to enhance the transport based on the mixing length argument, it can limit the saturation amplitude of fluctuations so that the turbulent transport may be low.*

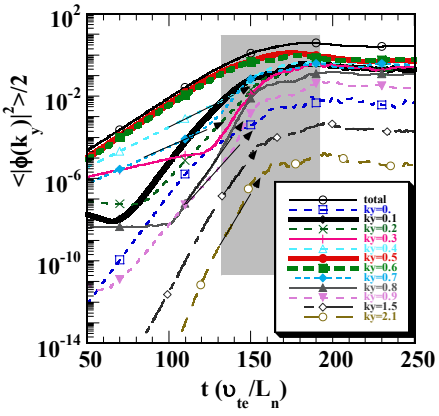

Fig.9 Time evolution of 3D slab ETG potential energy. The direction of the arrows marks an exponentially growing tendency. $\eta_e = 6$, $\hat{s} = 1.4$, $\mu_\perp = 0.5$, $L_x = 50\rho_e$, $L_y = 20\pi\rho_e$, $L_z = 2\pi L_n$.

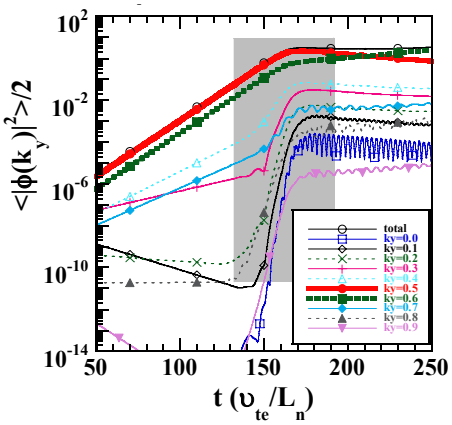

Fig.10 Time evolution of 2D linear slab ETG potential energy with an external streamer $\phi_s = 0.1|\phi(t)_{ky=0.5}\phi(t)_{ky=0.6}|\cos(0.1y)$. $\eta_e = 6$, $\hat{s} = 1.4$, $\mu_\perp = 0.5$, $L_x = 50\rho_e$, $L_y = 20\pi\rho_e$.

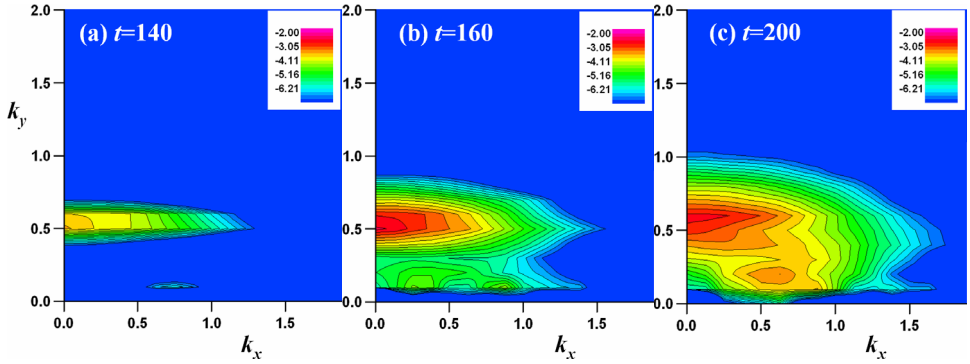

Fig.11 Time evolution of spectral distribution $\ln(<\phi^2(k_x,k_y)>_t/2)$ *of potential energy in* k_x-k_y *plane before(a), pre-saturation(b) and post-saturation(c) in the 3D simulation of Fig.9.*

4. Effects of Wave-type Mean Flow on ETG Zonal Flow Generation

Multiple spatial-temporal scale turbulence involves complicated cross-scale interaction processes. While short wavelength ETG zonal flows interplay with ITG fluctuation through nonlocal mode coupling[4], the smooth mean shear flow driven by neoclassical mechanism or MHD fluctuation can reduce the growth rate of zonal flow generation in ITG turbulence. Here the process of a large-scale wave-type mean flow interplaying with the microscopic turbulence is studied. As an example, the ITG zonal flow sampled as the wave-type mean flow is externally imposed in ETG turbulence to understand the role of different type sheared flows in the generation of zonal flows. In this case, the radial dependence of the wave-type mean flow is modeled by a sinusoidal or cosinusoidal function with negligible shearing rate. The analyses are carried out with two steps based on HM turbulence. A nine-wave coupling model, which includes additional coupling between the wave-type mean flow and the sidebands of the usual 4-wave modulational interaction, is first developed to calculate the effect on the growth rate of ETG zonal flows[24]. Obvious reduction of the growth rate of ETG zonal flow is observed, similar to the effect of smooth mean flow on ITG zonal flow generation based on the analysis of wave kinetic equation[8]. The reduction of the growth rate results from the increase of real frequency so that the zonal flow resonance becomes less satisfied due to the frequency mismatch condition. However, this simplified modeling has ignored the direct mode coupling between the wave-type mean flow and the pump waves, which may modify the spectral distribution of pumping force. Numerically solving the complete coupling system based on HM model shows a very slight stabilization of ETG zonal flow generation due to the wave-type mean flows. It is found that the wave-type mean flow mainly scatters the pump wave to have a spectral distribution under the energy conservation. The overall effect of the wave-type mean flow on the ETG zonal flow generation from the two sets of coupling seems to approximately cancel each other out so that the zonal flow generation mainly depends on the total pump wave energy.

5. Summary and Conclusion

3D ETG and ITG turbulence simulations as well as 2D modeling analysis have clearly shown the key role of nonlinear mode coupling in the dual interaction processes of the dynamics of secondary structures in turbulence. Coherent large-scale flow structures can behave as a stationary wave, namely *wave-type flow*, in multiple scale turbulence and interplay with fluctuations through ubiquitous nonlinear mode coupling, inducing possible decay of the turbulence. Main results are

obtained in three aspects: (1) The back-action of secondary anisotropic large-scale flow structures on ETG or ITG turbulence through mode coupling can deform Kolmogorov-type power-law spectrum into an exponential-law scaling in the inertial region; (2) Streamer-like long wavelength structure can saturate linear slab ETG mode only through the mode coupling with the most unstable components. It is observed that secondary long wavelength fluctuation in ETG fluctuations may saturate ETG turbulence through a similar mechanism. (3) A wave-type mean flow with negligible shearing rate can scatter the pump wave energy to have a wider spectrum through mode coupling, but it seems to have less effect on the zonal flow generation in HM turbulence.

Acknowledgements:
One of authors (J. Li) acknowledges helpful discussion with L. Chen, P. Diamond and H. Sanuki. He would like to thank M. Azumi, H. Ninomiya, M. Kikuchi and Y. Liu for support. This work was partly carried out in Southwestern Institute of Physics (SWIP), China and Graduate School of Energy Science, Kyoto University, Japan. The simulations were partially performed in Japan Atomic Energy Research Agency (JAEA), Naka and University of California, Irvine (UCI) when J. Li visited there. This work was partially supported by National Natural Science Foundation of China (NFSC) Grants No. 10575032 and No. 10575031 and by the JSPS-CAS (Japan–China) Core University Program on Plasma and Nuclear Fusion.

References

1. S.-I. Itoh and K. Itoh. Plasma Phys. Control. Fusion 43, 1055(2001)
2. F. Jenko, B.Scott, et al. 19th IAEA Fusion Energy, IAEA-CN-94/TH/1-2, 2002
3. Y. Kishimoto, Jiquan Li, et al. 19th IAEA Fusion Energy, IAEA-CN-94/TH/1-5, (2002)
4. Jiquan Li and Y. Kishimoto, Phys. Rev. Lett. 89, 115002(2002)
5. C. J. McDevitt and P. H. Diamond, Phys. Plasmas **13**, 032302 (2006)
6. L. Chen, Z. Lin and R. White, Phys. Plasmas 7, 3129(2000)
7. A. I. Smolyakov, P. H. Diamond and V. I. Shevchenko, Phys. Plasmas 7, 1349(2000)
8. E. Kim and P. Diamond, Phys. Plasmas 10, 1698(2003)
9. J.A. Krommes and C. B. Kim, Phys. Rev. E 62, 8508(2000)
10. S. Champeaux and P. Diamond, Phys. Lett. A 288, 214(2001)
11. W. Dorland, F. Jenko, et al., Phys. Rev. Lett. 85,5579(2000);Phys. Plasmas 7,1904(2000)
12. Jiquan Li and Y. Kishimoto, et al. Nucl. Fusion 45, 1293(2005)
13. T.S. Hahm, and K. H. Burrell, Phys. Plasmas 2, 1648(1995)
14. P. Diamond, S. Champeaux, *et al*., Nucl. Fusion 41, 1067(2001)
15. C. Holland, P. Diamond, et al., Nucl. Fusion 43, 761(2003)
16. Z. Lin, L. Chen, F. Zonca, Phys. Plasmas 12, 056125(2005)
17. L. Chen, F. Zonca, Z. Lin, Plasma Phys. Control. Fusion 47, B71 (2005)
18. A.Hasegawa and K. Mima, Phys. Fluids 21,87(1978)
19. W. Horton, et al. Phys. Fluids 31, 2971(1988)
20. Jiquan Li and Y. Kishimoto, Phys. Plasmas 11, 1493(2004)
21. J.L.Ottinger and D. Carati, Phys. Rev. E 48, 2955(1993)
22. B. Labit and M. Ottaviani, Phys. Plasmas **10**, 126 (2003)
23. Y. Idomura, et al. 20th IAEA Fusion Energy, IAEA-CN-116/TH/8-1, 2004
24. K. Uzawa, Y.Kishimoto and Jiquan Li, Plasmas & Fusion Res. 1, 024(2006)